2001 International Conference on Indium Phosphide and Related Materials
Conference Proceedings
13th IPRM 14-18, May 2001 Nara, Japan

FIRST InP/InGaAs PNP HBT GROWN BY METAL ORGANIC CHEMICAL VAPOR DEPOSITION

Delong Cui, Shawn Hsu and Dimitris Pavlidis
Department of Electrical Engineering and Computer Science, The University of Michigan, Ann Arbor, MI 48104, USA
Phone: 1-734-647-1778, Fax: 1-734-763-9324, E-mail: pavlidis@umich.edu

Abstract

The MOCVD growth of InP/InGaAs PNP HBT layers and the successful fabrication and operation at high frequency of devices made on such layers are reported for the first time. The PNP HBTs employed a zinc-doped InP layer as emitter while the base was made with a 500Å thick n-type InGaAs layer doped at $5\times10^{18}cm^{-3}$. Microwave measurements indicated f_T of more than 11 GHz at $J_C=8.25\times10^4$ A/cm^2 for these MOCVD-grown InP/InGaAs PNP HBTs.

Introduction

InP-based HBTs have demonstrated excellent current-handling capability and superior frequency performance. While research of InP-based HBTs has almost exclusively focused on NPN HBTs because electron velocity is several orders of magnitude higher than the hole velocity in InGaAs material, InP-based PNP HBTs have recently attracted interest, primarily due to the possibility of their integration in circuits with their NPN counterparts. PNP HBTs can be used as active loads for NPN HBTs and allow the design of multi-stage amplifiers with alternating NPN and PNP HBTs. Moreover, integrated NPN and PNP HBTs can form class B push-pull power amplifiers for simultaneous improvement of both efficiency and linearity.

While there have been a number of reports on InAlAs/InGaAs PNP HBTs [1]-[7], little has been reported on InP/InGaAs PNP HBTs due to the difficulty in obtaining high p-type concentration in the emitter while keeping a low p-type concentration in the collector. To the author's knowledge, the only InP/InGaAs PNP HBT reported so far was grown by MOMBE and demonstrated a gain of 20 and f_T, f_{max} of 10.5GHz, 25 GHz respectively for HBTs with $3\times8\mu m^2$ emitters [8].

In this paper, we report for the first time the successful growth and fabrication of InP/InGaAs PNP HBTs grown by Metal Organic Chemical Vapor Deposition (MOCVD). InP/InGaAs PNP HBTs have been fabricated using a self-aligned, all wet-etch based technology developed in the University of Michigan. $1\times20\mu m^2$ HBTs showed DC gain of more than 10 with f_T of 11.2 GHz.

MOCVD Growth and Device Fabrication

The HBTs were grown on (001) semi-insulating InP substrates in a modified EMCORE GS3200 low pressure Metal Organic Chemical Vapor Deposition system (LP-MOCVD). The pressure of the growth chamber was maintained at 60torr and the susceptor was rotated at 100rpm to provide the best sample uniformity. The group III metalorganics used in this study were all-methyl organometallic precursors: trimethylindium (TMIn) and trimethylgallium (TMGa). 100% pure AsH_3 and PH_3 were used for group V precursors. DeZn and Si_2H_6 were used as p-type and n-type dopants respectively.

The InP/InGaAs HBT structure is shown in Table 1. It is composed of a 5000Å p^+-InGaAs subcollector, 3000Å p^--InGaAs collector, 500Å n^+-InGaAs base, 100Å undoped InGaAs spacer, 1500Å P-InP and 700Å P^+-InP as emitter, and a 2000Å p^+-InGaAs emitter cap layer. The growth was carried out at a growth temperature of 570°C.

Layer	Type	Thickness (Å)
Emitter Cap	p^+-InGaAs	2000
	P^+-InP	700
Emitter	P-InP	1500
Spacer	i-InGaAs	100
Base	n^+-InGaAs	500
Collector	p^--InGaAs	3000
Subcollector	p^+-InGaAs	5000
Substrate	Semi-Insulating InP (001)	

Table 1: MOCVD-Grown PNP InP/InGaAs HBT Structure

HBTs were fabricated by using a self-aligned, all wet etch-based process developed in the University of Michigan. The base contacts were self-aligned to the emitters to reduce the base parasitic resistance. The emitters were protected and the wafers were then etched to the sub-collector layer using the base contact as etch mask after base metallization. The p-type metal used in this study was Pt/Ti/Pt/Au and the n-type metal was Ti/Pt/Au. After each p-type metallization, the ohmic contacts were optimized by annealing the wafer at 375°C for 7 seconds using Rapid Thermal Annealing (RTA) to improve the ohmic contact conductivity.

Device Measurements Results and Discussion

Fig. 1 shows the common-emitter I_C-V_{EC} characteristics for the fabricated MOCVD-grown PNP InP/InGaAs

0-7803-6700-6/01/$10.00 ©2001 IEEE

HBTs with $1\times20\mu m^2$ emitter geometry. As can be seen, at I_B=0.6mA, the collector currents were 3.6mA and 5.5mA at V_{EC}=1.0V and 1.5V respectively, corresponding to an Early voltage of 0.85V. This is a direct result of the thin base width (500Å), which leads in base width decrease and the strong presence of Early effects, as the emitter-collector voltage increases. The gain increased rapidly as the emitter-collector voltage V_{EC} increased. For example, at V_{EC}=1.5V, I_B=0.6mA, the beta of the measured transistor was 9 while a beta of 28 was found at V_{EC}=3.0V, I_B=0.6mA.

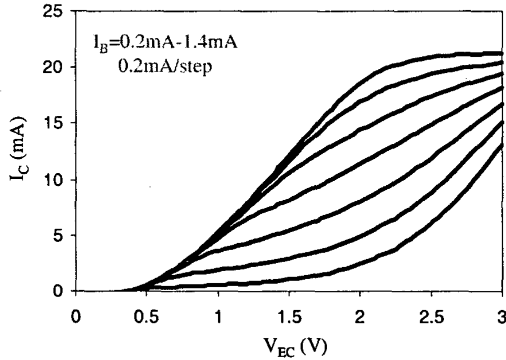

Fig. 1: Forward I-V characteristics of $1\times20\mu m^2$ MOCVD-grown InP/InGaAs PNP HBTs

However, due to the base push-out, the transistor gain reduced sharply as the collector current/base current increased. Fig. 2 illustrates beta as a function of emitter-collector voltage and base current. There are two features noticed, first the gain increased as the emitter-collector voltage increased, for example, at I_B=0.6mA, beta increased from 9.0 at V_{EC}=1.5V to 28.0 at V_{EC}=3.0V. This is attributed to the small Early voltage (V_A~0.85V) due to the thin base width. It is also noticed that the gain compressed very rapidly as the base current/collector current increased. As can be seen, beta at V_{EC}=3.0V decreases from 28 at I_B=0.6mA to 17.2 at I_B=1.2mA. This shows strong base push-out effects of the PNP InP/InGaAs transistor and is a direct result of the short diffusion length of the holes.

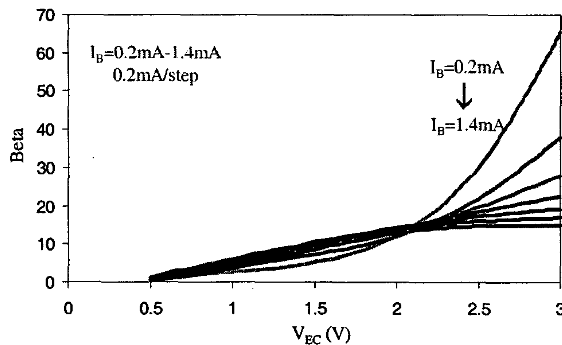

Fig. 2 Beta as a function of V_{EC} and I_B for 1×20 μm^2 PNP InP/InGaAs HBT

The Gummel plot of a 1×20 μm^2 PNP InP/InGaAs HBT is shown in Fig. 3. The ideality factors for collector current and base current were 1.3 and 2.5 respectively. The large base ideality factor suggested that there is also considerable amount of recombination in the base-emitter space charge region, the depleted spacer and/or along the external surfaces of the emitter mesa. A considerable presence of base leakage current was found, which may to a great extent have been introduced by the fact that the band discontinuity appears primarily in the valence rather than conduction band ($\Delta E_C/\Delta E_V$~250meV/340meV) between InP and InGaAs. As a comparison, the conduction band discontinuity in InAlAs/InGaAs is approximately 480meV ($\Delta E_C/\Delta E_V$~480meV/240meV) as compared with 250meV conduction band discontinuity in InP/InGaAs.

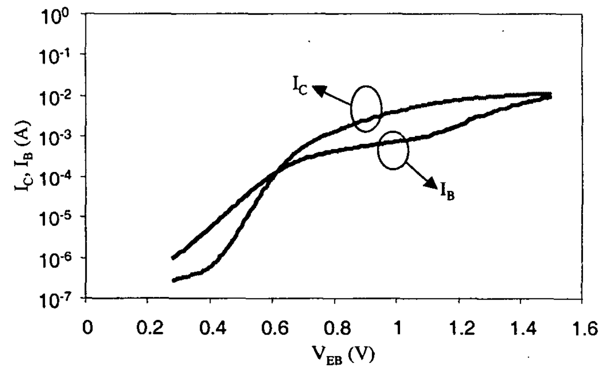

Fig. 3 Gummel plot of 1×20 μm^2 PNP InP/InGaAs HBT

Fig. 4 shows the current gain as a function of collector current density for a PNP InP/InGaAs HBT grown by MOCVD. The differential current gain h_{fe} was larger than large-signal current gain h_{FE}. This is a direct result of larger base current ideality factor than collector current ideality factor $n_B>n_C$ as the current gain increases with I_C. For example, the peak h_{fe} was 11 while the peak h_{FE} was about 6.

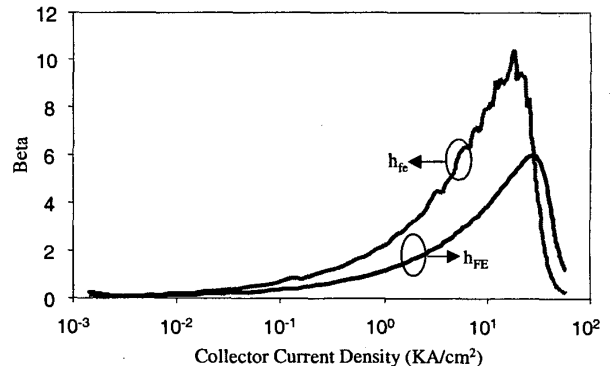

Fig. 4 h_{fe} and h_{FE} current gain as a function of current density for $1\times20\mu m^2$ PNP InP/InGaAs HBT

It should be noticed at this point that the general Gummel plot measurement reported earlier was performed under conditions of $V_{EC}=V_{EB}$. The current gain could consequently be significantly higher at larger V_{EC}, as already illustrated by the results of Fig. 1 and Fig. 2. Fig.4 also shows that both the differential and large-signal current gain decrease sharply at collector current density larger than 20-30 kA/cm^2. This is due to the significant base push-out when the collector current density exceeds the critical value of 20kA/cm^2.

The small signal S-parameters of MOCVD-grown PNP InP/InGaAs HBTs were measured by using an HP8510B network analyzer from 0.5GHz to 25.5 GHz. The current gain $|h_{21}|^2$, maximum power gain G_{max} were calculated from the measured S-parameters and plotted in Fig. 5 for a 1×20μm^2 HBT.

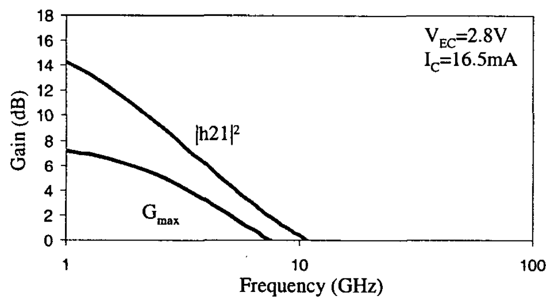

Fig. 5 Microwave performance of a 1×20μm^2 MOCVD-grown PNP HBT at I_C=16.5mA and V_{EC}=2.8V.

Fig. 5 shows the microwave performance of a 1×20μm^2 MOCVD-grown PNP HBT. f_T and f_{max} were found to be 11.2 GHz and 8.1 GHz respectively at the optimum biasing condition of V_{EC}=2.8Vand I_C=16.5mA.

As can be seen from the above discussion, the DC gain (β=28) of MOCVD-grown PNP InP/InGaAs HBTs was similar to that of MOMBE-grown devices (β=20) [8]. While the f_T performance was also comparable with that of similar designs grown by MOMBE (f_T=10.5 GHz) [8], the f_{max} performance was considerably lower (f_{max}=25GHz) [8]. This is due to the limitation of minimum controllable p-type doping concentration in the MOCVD growth system used for growth of these device layers. A minimum p$^-$ collector doping concentration of high 10^{17} cm^{-3} was possible in the system instead of the desirable value of 10^{16} cm^{-3}. For example, the collector doping concentration was 1×10^{16}cm^{-3} in MOMBE-grown PNP HBTs [8]. It is well known that a convenient approximate expression for f_{max} is:

$$f_{max} = \left(\frac{f_T}{8\pi R_B C_{BC}}\right)^{1/2} \tag{1}$$

where R_B is the parasitic base resistance and C_{BC} is the base-collector capacitance. As can be seen from Eq. (1), f_{max} is approximately inversely proportional to the square root of base-collector capacitance. The undesirable high collector doping concentration (high 10^{17} cm^{-3}) compared with the designed value of 10^{16} cm^{-3} introduced less depletion width in collector region and therefore increased the base-collector capacitance considerably.

Further improvement in f_{max} performance is expected to be feasible by controlling the doping concentration of the collector. For example, by decreasing the minimum controllable p-type doping concentration of InGaAs material to 10^{16}cm^{-3}, one can significantly increase the depletion width in collector layer and hence increase the f_{max} performance. An f_{max} performance of ~25GHz, similar to that of MOMBE grown devices is expected if the collector doping concentration is decreased to ~10^{16}cm^{-3}.

From the f_T and f_{max} measurements, the sum of base transit time and the collector charging time can be estimated [9]. The total emitter-to-collector delay τ_{ec} is:

$$\tau_{ec} = \frac{1}{2\pi f_T} = \tau_e + \tau_b + \tau_{pcd} + \tau_c$$

$$= \frac{kT}{qI_E}C_{BE} + \left(\frac{W_B^2}{2D_p} + \frac{W_B}{2v_{bc}}\right) + \frac{W_c}{2v_c} + \left(R_c + R_E + \frac{kT}{qI_E}\right)C_{BC}$$

$$= \frac{1}{I_E}\left(\frac{kT}{q}C_{BE} + \frac{kT}{q}C_{BC}\right) + \left[\left(\frac{W_B^2}{2D_p} + \frac{W_B}{2v_{bc}}\right) + \frac{W_c}{2v_c} + (R_c + R_E)C_{BC}\right] \tag{2}$$

where τ_e, τ_b, τ_{pcd}, and τ_c are the emitter charging, base transit, pre-collector delay, and collector charging times; W_B is the neutral base width; W_C is the collector depletion width; v_{bc} is the velocity with which electrons are swept into the base collector depletion region; v_c is the average electron velocity in the collector.

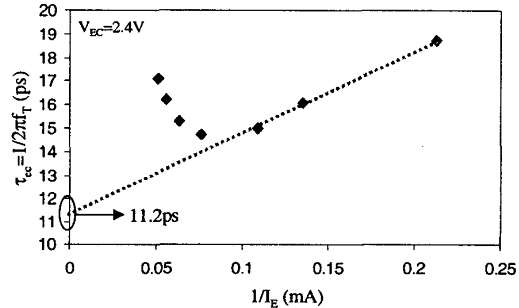

Fig. 6 Plot of τ_{ec} versus $1/I_E$ for PNP InP/InGaAs HBTs grown by MOCVD

Fig. 6 shows the total transit time from emitter to collector τ_{ec} as a function of the reciprocal of the emitter current for a 1×20μm^2 PNP HBT with V_{EC}=2.4V. One can see that τ_{ec} follows the linear relationship with $1/I_E$ at low current levels. At high current levels, due to the Kirk effects, the effective W_B and C_{BC} increase and therefore τ_{ec} increases as a result.

By extrapolating the region where τ_{ec} follows linear relationship with $1/I_E$, one can find τ' at $1/I_E$=0,

$$\tau' = \left(\frac{W_B^2}{2D_p} + \frac{W_B}{v_{bc}}\right) + \frac{W_c}{2v_c} + (R_c + R_E)C_{BC} \tag{3}$$

while Q_d, the slope of the curve, is given by:

$$Q_d = \frac{kT}{q}C_{BE} + \frac{kT}{q}C_{BC} \tag{4}$$

The sum of base transit time and the collector charging time τ' at $1/I_E=0$ was found to be 11.2 ps. This almost accounts for 75% of the total emitter to collector delay time which was 15.0ps under the biasing condition of $I_E=9.2mA$. It indicates that the base transit time and the collector charging time dominate the high frequency performance of the InP/InGaAs PNP transistor, while other components such as emitter charging time and pre-collector delay time only account for 25% of the total emitter to collector delay time.

The above results indicate that the high frequency performance of InP/InGaAs PNP HBTs is to a great extent limited by the use of uniformly doped InGaAs base. Compositionally graded base [10] and doping graded base designs [11] have been employed in AlGaAs/GaAs material system to improve the high speed performance of the PNP AlGaAs/GaAs HBTs. Similar approaches can be applied to InP/InGaAs PNP HBTs, where the introduction of electrical fields into the n-type base region could aid the hole transition through the base and reduce the total emitter to collector transit time significantly.

Improvement is also expected by decreasing the collector doping concentration as for example obtained by lowering the minimum controllable p-type doping concentration from high $10^{17}cm^{-3}$ to $10^{16}cm^{-3}$ [8]. This could reduce the base-collector capacitance by increasing the collector depletion width. As a result, the f_{max} performance could be improved significantly over the present characteristics which are limited by the lowest controllable p-type doping concentration of the present growth system.

Conclusion

Overall, PNP InP/InGaAs HBTs have been grown by metal organic chemical vapor deposition (MOCVD) for the first time. An all wet-etch based process has been used to fabricate PNP HBTs from these layers. Successful high frequency operation has been demonstrated. Gain of more than 10 and f_T of 11.2 GHz have been achieved for HBTs with $1\times20\mu m^2$ emitter geometries. The relatively low f_{max} performance (8.1GHz) has been attributed to the limitation of the minimum controllable p-type doping concentration for InGaAs material in the present MOCVD system. It has also been pointed out that the base transit time and collector charging time dominated the high frequency performance of the MOCVD-grown PNP transistors. Both compositional and doping gradient could be introduced into the base region to provide an electrical field to accelerate the holes and improve the overall high frequency performance.

Acknowledgements

This work is supported by ARO MURI (DAAH04-96-1-0001).

Reference

[1] D. Sawdai, X. Zhang, D. Pavlidis, and P. Bhattacharya, "Performance Optimization of PNP InAlAs/InGaAs HBTs," *Proc. IEEE/Cornell Conf. On Advanced Concepts in High Speed Semiconductor Devices and Circuits,* PP. 269-277, 1997.

[2] D. Sawdai, X. Zhang, D. Pavlidis, and P. Bhattacharya, "Power Performance of PNP InAlAs/InGaAs HBTs," *10th Int. Conf. InP and Related Materials,* pp. 72-75, 1998.

[3] D. Sawdai, X. Zhang, D. Pavlidis, and P. Bhattacharya, "Properties of Fully Self-Aligned InAlAs/InGaAs PNP HBTs with Very Thin Bases," *11th Int. Conf. InP and Related Materials,* pp. 187-190, 1999.

[4] W. Stanchina, R. A. Metzger, M. W. Pierce, J. F. Jensen, L. G. McCray, R. Wong-Quan, and F. Williams, "Monolithic Fabrication of NPN and PNP AlInAs/GaInAs HBTs," 5th Int Conf InP and Related Materials, pp. 569-571, 1993

[5] T. Won, C. Peng, J. Chyi, and H. Morkoc, "$In_{0.52}Al_{0.48}As/In_{0.53}Ga_{0.47}As$ Double Heterojunction p-n-p Bipolar Transistors Grown by Molecular Beam Epitaxy," *IEEE Electron Dev Lett,* Vol. 9, pp. 334-336, 1988.

[6] A. NaKagawa and K. Inoue, "Symmetric P-n-P InAlAs/InGaAs Double Heterojunction Bipolar Transistors Fabricated with Si-Ion Implantation," *IEEE Electron Dev Lett.* Vol. 13, pp. 285-287, 1992.

[7] P. Parikh, K. Kiziloglu, M. Mondry, P. Chavarkar, B. Keller, S. Denbarrs, and u. Mishra, "InP-Based Devices and Their Applications for Merged FET-HBT Technolgies," *Microwave and Optical Technology Letters,* Vol. 11, pp. 121-125, Feburary 20, 1996.

[8] L.M. Lunardi, S. Chandrasekhar, and R. A. Hamm, "High-Speed, high-Current-Gain P-n-P InP/InGaAs Heterojunction Bipolar Transistors," *IEEE Electron Dev Lett,* Vol. 14, pp. 19-21, 1993.

[9] D. Slater, P. Enquist, F. Najjar, M. Chen, J. Hutchby, A. Morris, and R. Trew, "Experimental Values for the Hole Diffusion Coefficient and Collector Transit Velocity in P-n-P AlGaAs/GaAs HBTs," *IEEE Electron. Dev. Lett.,* Vol. 12, pp. 54-56, 1991.

[10] A. Kameyama, A. Massengale, C. Dai, and J. Harris, "Aluminum-Graded-Base PNp AlGaAs/GaAs Heterojunction Transistor with 37 GHz Cut-Off Frequency," *IEICE Trans Electronics,* Vol. E79-C, pp. 518-523, April 1996.

[11] D. Hill, T. S. Kim, and H. Q. Tseng, "X-band Power AlGaAs/InGaAs P-n-p HBTs," *IEEE Electron Dev Lett,* Vol. 14, pp. 185-187, April 1993.